Respiratory Physiology & Neurobiology 265 (2019) 55–67

Contents lists available at ScienceDirect

Respiratory Physiology & Neurobiology

journal homepage: www.elsevier.com/locate/resphysiol

No evidence in support of a prodromal respiratory control signature in the TgF344-AD rat model of Alzheimer's disease

Eric F. Lucking[a], Kevin H. Murphy[a], David P. Burns[a], Anirudh V. Jaisimha[b], Kevin J. Barry-Murphy[a], Pardeep Dhaliwal[a], Barry Boland[b], Mark G. Rae[a], Ken D. O'Halloran[a,*]

[a] Department of Physiology, School of Medicine, College of Medicine & Health, University College Cork, Cork, Ireland
[b] Department of Pharmacology and Therapeutics, School of Medicine, College of Medicine & Health, University College Cork, Cork, Ireland

ARTICLE INFO

Keywords:
Amyloid precursor protein
Presenilin-1
Respiratory behaviour
Neuroinflammation
Pulmonary chemoreflex

ABSTRACT

Alzheimer's disease (AD) is a progressive neurodegenerative condition disturbing major brain networks, including those pivotal to the motor control of breathing. The aim of this study was to examine respiratory control in the TgF344-AD transgenic rat model of AD. At 8–11 months of age, basal minute ventilation and ventilatory responsiveness to chemostimulation were equivalent in conscious wild-type (WT) and TgF344-AD rats. Under urethane anesthesia, basal diaphragm and genioglossus EMG activities were similar in WT and TgF344-AD rats. The duration of phenylbiguanide-induced apnoea was significantly shorter in TgF344-AD rats compared with WT. Following bilateral cervical vagotomy, diaphragm and genioglossus EMG responsiveness to chemostimulation were intact in TgF344-AD rats. Amyloid precursor protein C-terminal fragments were elevated in the TgF344-AD brainstem, in the absence of amyloid-β accumulation or alterations in tau phosphorylation. Brainstem pro-inflammatory cytokine concentrations were not increased in TgF344-AD rats. We conclude that neural control of breathing is preserved in TgF344-AD rats at this stage of the disease.

1. Introduction

Alzheimer's disease (AD), a neurodegenerative disease profoundly linked with dementia, is characterised by aggregation of amyloid-β (Aβ) plaques and neurofibrillary tangles. The resultant synaptic defects manifest in cognitive dysfunction, the hallmark feature of this devastating disease. Post-mortem analysis of AD patients reveals the presence of Aβ plaques and neurofibrillary tangles in the hindbrain (Simic et al., 2009). Indeed, it has been postulated that the neurodegenerative advancement of AD may originate in the brainstem (Simic et al., 2009). It is well established that chronic neuroinflammation presents in AD patients (Akiyama et al., 2000; Heneka et al., 2015; Van Eldik et al., 2016), with therapeutic agents for cognitive improvement acting to decrease pro-inflammatory cytokines (Kokras et al., 2018). In AD patients, Aβ plaques activate microglia resulting in the production of pro-inflammatory cytokines such as tumour necrosis factor-α (TNF-a), interleukin-1 (IL-1) and IL-6 (Lue et al., 2001).

Animal models of AD present with altered motor control of upper airway function essential for vocalisation, swallowing and maintenance of airway patency (Dutschmann et al., 2010; Menuet et al., 2011b). Dutschmann et al. (2010) reported increased airway resistance in an aged transgenic mouse model of AD. Dysregulated motor output to laryngeal constrictor muscles contributed to altered control of respiratory airflow, which was compensated by way of an increase in chest movement during eupnoeic breathing (Dutschmann et al., 2010). Larger inspiratory chest movements are required to sufficiently ventilate the lungs, increasing respiratory work and metabolic demand during eupnoea. In the later stages of disease in this animal model of AD, respiratory rhythm is abnormal as a result of dysfunction at the level of respiratory centres, with evidence of tauopathy in the nucleus tractus solitarius (NTS) (Menuet et al., 2011a).

The NTS has important outputs to hypoglossal motor neurons (Borke et al., 1983), which in turn regulate the genioglossus, the principal upper airway dilator muscle pivotal in the control of airway calibre. Sleep disordered breathing (SDB) is associated with reduced neural drive to the upper airway muscles (Borel et al., 2016), predisposing the pharyngeal airway to collapse. Thus, it is plausible to suggest that brainstem dysfunction in AD patients could explain the increased

Abbreviations: 5-HT, 5-hydroxytryptamine (serotonin); Aβ, amyloid-β protein; AD, Alzheimer's disease; APP, amyloid precursor protein; APP_{SWE}, Swedish mutant human amyloid precursor protein; CTF, C-terminal fragments; EMG, electromyography; f_R, respiratory frequency; IFN-y, interferon-y; IL, interleukin; KC/GRO, keratinocyte chemoattractant/growth related oncogene; NTS, nucleus tractus solitarius; PS1ΔE9, presenilin-1; SDB, sleep-disordered breathing; TNF-α, tumour necrosis factor; V_E, minute ventilation; V_T, tidal volume; WT, wild type

* Corresponding author at: Department of Physiology, Western Gateway Building, Western Road, Cork, Ireland.
E-mail address: k.ohalloran@ucc.ie (K.D. O'Halloran).

https://doi.org/10.1016/j.resp.2018.06.014
Received 29 March 2018; Received in revised form 25 May 2018; Accepted 29 June 2018
Available online 30 June 2018
1569-9048/ © 2018 Elsevier B.V. All rights reserved.

Table 1
Baseline Ventilation in Conscious Wild-Type and TgF344-AD Rats.

	Wild-type		TgF344-AD		
	Male (n = 8)	Female (n = 12)	Male (n = 9)	Female (n = 12)	Two-way ANOVA
f_R (bpm)	81 ± 10	81 ± 10	85 ± 8	72 ± 9$^{\$}$	Gene: p = 0.452; Sex: p = 0.04; Interaction: p = 0.048
V_T (ml/100 g)	0.50 ± 0.07	0.66 ± 0.09*	0.47 ± 0.03	0.70 ± 0.20$^{\$}$	Gene: p = 0.884; Sex: p < 0.001; Interaction: p = 0.268
V_E (ml/min/100 g)	38.8 ± 6.2	50.3 ± 7.6*	38.0 ± 3.3	47.8 ± 11.1$^{\$}$	Gene: p = 0.534; Sex: p < 0.001; Interaction: p = 0.738
Body mass (g)	372 ± 64	234 ± 63	421 ± 33	230 ± 17$^{\$}$	Gene: p = 0.141; Sex: p < 0.001; Interaction: p = 0.089

f_R, respiratory frequency; V_T, tidal volume; V_E, minute ventilation. Data are shown as mean ± SD and were statistically compared by two-way ANOVA (gene x sex) with Bonferroni *post hoc* test. * Wild-type female versus wild-type male, p < 0.05; $ TgF344-AD female versus TgF344-AD male, p < 0.05.

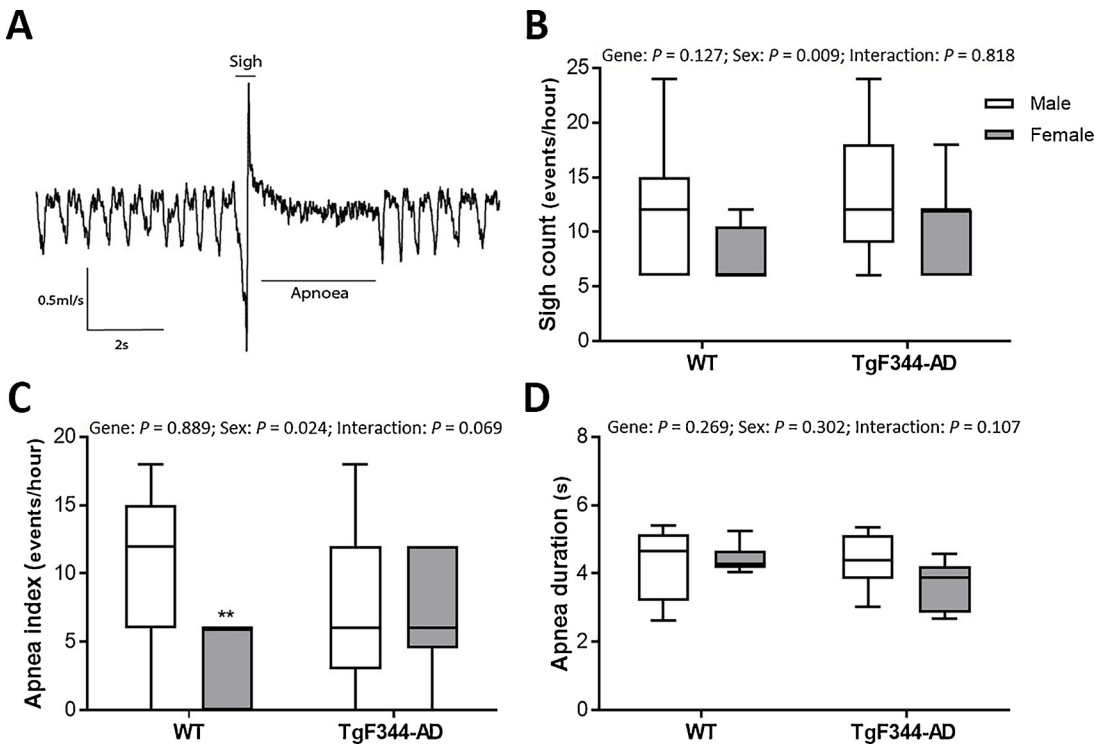

Fig. 1. Apnoeas and augmented breaths in conscious wild-type and TgF344-AD rats.
A) Representative respiratory flow trace (inspiration downward) illustrating a sigh (augmented breath) followed by an apnoea (cessation of flow) in a TgF344-AD animal. Group data shows frequency of augmented breaths per hour (B), apnoeas per hour (C) and the average duration of apnoeas (D). WT, wild type. Values (B–D) are expressed as box and whisker plots (median, 25–75 percentiles and minimum and maximum values). Groups were statistically compared by two-way ANOVA (gene x sex) with Bonferroni *post hoc* test. **WT female versus WT male, p < 0.01.

risk for SDB development (Daulatzai, 2013; Emamian et al., 2016). Intermittent hypoxia, a hallmark feature of SDB, independently increases central nervous system tauopathy (Yagishita et al., 2017), accelerates the onset of cognitive decline in AD (Osorio et al., 2015; Pan and Kastin, 2014), is deleterious to the control of breathing (McDonald et al., 2015; O'Halloran, 2016; Skelly et al., 2012) and is independently associated with cardiovascular disease (Lucking et al., 2014; Marin et al., 2005; Souza et al., 2015), which is a risk factor for the development of AD (Newman et al., 2005). Thus, aberrant cardiorespiratory function is a potential driver of AD, with a potential pathogenic interplay between AD and impaired respiratory control. Moreover, impaired upper airway function results in dysphagia (Boccardi et al., 2016; Manabe et al., 2017; Mitchell et al., 2009; Secil et al., 2016; van der Steen et al., 2006) and the aspiration of ingested materials, which subsequently leads to respiratory infections such as pneumonia, the most prevalent cause of death in patients with dementia (Manabe et al., 2017; Mitchell et al., 2009; van der Steen et al., 2006). Eliminating dysphagia-induced aspiration via tube feeding in patients with dementia reduces the frequency of pneumonia and prolongs survival (Takenoshita et al., 2017).

There remains a paucity of studies exploring the cardiorespiratory consequences of AD-related neurodegeneration, despite the potential relevance to disease progression and the possibility of identifying prodromal features that inform the clinical management of patients with AD. We therefore sought to explore respiratory behaviour in a novel rat model of Alzheimer's disease (TgF344-AD), seeking to characterise breathing and motor control of the upper airway, together with the assessment of amyloid precursor protein (APP) metabolism and cytokine concentrations in the brainstem. The TgF344-AD rat model recapitulates human AD pathology in an age-dependent manner (Cohen et al., 2013). This model, which manifests behavioural impairment, neuronal loss, amyloid plaques and tau pathology, is considered the

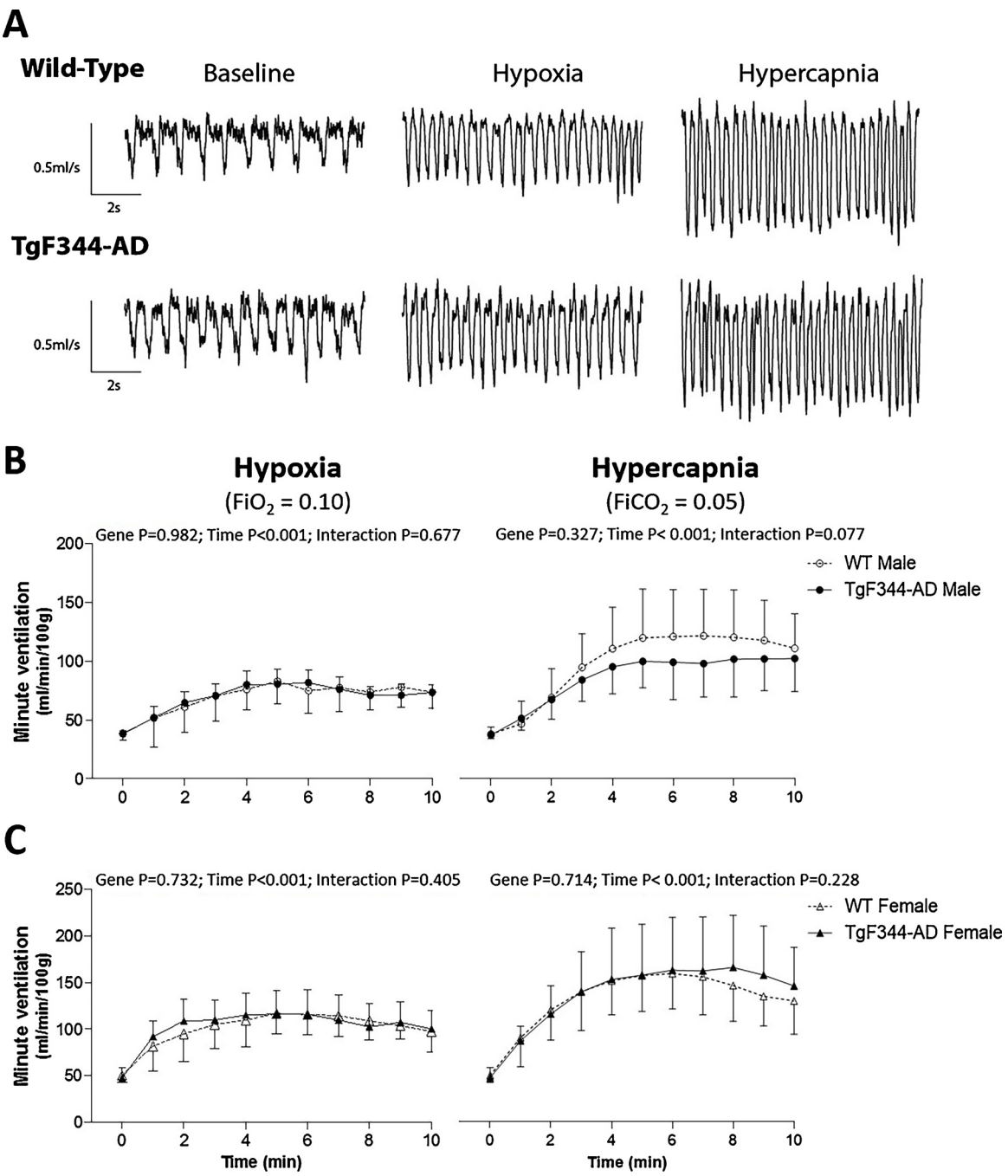

Fig. 2. Ventilatory responsiveness to hypoxia and hypercapnia in conscious wild-type and TgF344-AD rats.
A) Representative respiratory flow traces during baseline, hypoxic and hypercapnic breathing in wild-type and TgF344-AD rats. Group data (mean ± SD) showing the ventilatory response to a ten minute hypoxia challenge (left panels) and a ten minute hypercapnic challenge (right panels) in males (B) and females (C). WT, wild type. Groups were statistically compared by repeated measures two-way ANOVA (gene x time) with Bonferroni *post hoc* test.

most clinically appropriate rodent model of AD (Saraceno et al., 2013). We hypothesised that there would be evidence of a prodromal respiratory control signature in the TgF344-AD rat model of Alzheimer's disease.

2. Methods

2.1. Ethical approval

Procedures on live animals were performed under licence in strict accordance with Irish and European directive 2010/63/EU. Animal welfare and experimental protocols were approved by the Animal Experimentation Ethics Committee of University College Cork.

2.2. Animal model

We utilised male and female TgF344-AD rats containing the transgene integration of 'Swedish' mutant human APP (APP_{SWE}) and Δ exon 9 mutant human presenilin-1 (PS1ΔE9) (Cohen et al., 2013). TgF344-AD and non-transgenic wild-type (WT) rats were bred in our institution's animal facility and housed under age- and sex-matched conditions, maintained on a 12hr:12hr light/dark cycle with *ad libitum* access to water and food. Animals were studied at 8–11 months of age ensuring no age-bias between groups. Ear samples were used to confirm

Table 2
Baseline Cardiorespiratory and Arterial Blood Parameters in Anesthetised Wild-Type and TgF344-AD Rats.

	Wild-type		TgF344-AD		
	Male (n = 9)	Female (n = 9)	Male (n = 8)	Female (n = 12)	Two-way ANOVA
f_R (bpm)	88 ± 17	96 ± 10	81 ± 6	98 ± 16	Gene: p = 0.523; Sex: p = 0.011; Interaction: p = 0.334
V_T (ml/100 g)	0.41 ± 0.16	0.53 ± 0.17	0.36 ± 0.02	0.51 ± 0.10	Gene: p = 0.469; Sex: p = 0.005; Interaction: p = 0.733
V_E (ml/min/100 g)	35.7 ± 16.9	50.2 ± 14.3	29.1 ± 2.9	51.0 ± 18.8	Gene: p = 0.583; Sex: p = 0.001; Interaction: p = 0.478
MAP (mmHg)	83 ± 12	101 ± 18	84 ± 7	104 ± 14	Gene: p = 0.631; Sex: p < 0.001; Interaction: p = 0.8
HR (bpm)	388 ± 30	395 ± 28	402 ± 33	384 ± 41	Gene: p = 0.840; Sex: p = 0.578; Interaction: p = 0.244
PO_2 (mmHg)	103 ± 7	102 ± 6	113 ± 17	110 ± 12	Gene: p = 0.035; Sex: p = 0.59; Interaction: p = 0.801
PCO_2 (mmHg)	46.3 ± 6.9	52.4 ± 2.5*	47.6 ± 5.2	50.7 ± 4.3	Gene: p = 0.905; Sex: p = 0.013; Interaction: p = 0.392
pH	7.37 ± 0.05	7.34 ± 0.03	7.37 ± 0.03	7.33 ± 0.03	Gene: p = 0.411; Sex: p = 0.011; Interaction: p = 0.814
HCO_3^- (mmol/l)	26.5 ± 1.4	28.3 ± 1.0*	27.0 ± 1.3	26.4 ± 1.3	Gene: p = 0.126; Sex: p = 0.146; Interaction: p = 0.011
Haematocrit (%)	50 ± 2	52 ± 2	49 ± 2	50 ± 2	Gene: p = 0.011; Sex: p = 0.052; Interaction: p = 0.242
Haemoglobin (g/dl)	17.0 ± 0.7	17.7 ± 0.5	16.7 ± 0.5	16.9 ± 0.7	Gene: p = 0.014; Sex: p = 0.051; Interaction: p = 0.25

f_R, respiratory frequency; V_T, tidal volume; V_E, minute ventilation; MAP, mean arterial pressure; HR, heart rate; PO_2, partial pressure of oxygen; PCO_2, partial pressure of carbon dioxide; HCO_3^-, bicarbonate. Data are shown as mean ± SD and were statistically compared by two-way ANOVA (gene x sex) with Bonferroni *post hoc* test. *WT female versus WT male, p < 0.05.

animal genotypes by PCR for expression of APP_{SWE} and PS1ΔE9 genes. Researchers were blinded at all times to animal genotype during experimental recordings and data analysis. Genotype was confirmed post-mortem using ear samples.

2.3. Respiratory recordings in conscious wild-type and TgF344-AD rats

2.3.1. Whole-body plethysmography

Respiratory flow recordings were performed using whole-body plethysmography in unrestrained and unanesthetised rats during quiet rest. WT (male n = 8; female n = 12) and TgF344-AD (male n = 9; female n = 12) rats were introduced into paired plethysmograph chambers (Buxco Research Systems, Wilmington, NC, USA) and allowed a minimum one-hour acclimation period until the animal was sufficiently settled at quiet rest following typical exploration and grooming behaviours. Room air was passed through each chamber (2 L/min) ensuring the maintenance of optimal O_2 and CO_2 environmental conditions.

2.3.2. Experimental protocol

Subsequent to the acclimation period, a 20 min baseline recording was performed during normoxic breathing. This was followed by a 10 min hypoxic challenge (FiO_2 = 0.10; balance N_2). Following a minimum 30 min recovery period in normoxia and ensuring rats were settled post-hypoxia, a 20 min normoxic baseline period was recorded. This was followed by a 10 min hypercapnic challenge ($FiCO_2$ = 0.05; balance O_2). A patented algorithm incorporated into FinePoint™ software (Buxco Research Systems) was used to determine respiratory parameters including respiratory frequency (f_R), tidal volume (V_T), and minute ventilation (V_E), which were recorded on a breath-by-breath basis for analysis offline. Chamber temperature and humidity were continuously measured and utilised in the estimation of tidal volume. However, body temperature was not measured and was estimated at 37.5 °C for all groups. We acknowledge the limitation of this assumption noting that errors in the estimation of body temperature can introduce significant errors in the calculation of tidal volume. Moreover, rat body temperature can decrease in response to hypoxia, which would have implications for the accurate determination of tidal volume in our study. We assumed an equivalent body temperature in all animals and equivalent body temperature responses to hypoxia in all groups. For these reasons the ventilatory data derived by whole body plethysmography should be viewed with caution. We note however that plethysmography findings are generally consistent with the findings revealed by direct invasive measurement in anesthetised animals in our study.

2.3.3. Data analysis

Baseline normoxic breathing was determined as an average of the entire baseline period. For both the hypoxic and hypercapnic challenges, ventilatory measurements were averaged on a minute-by-minute basis for the duration of the challenge. V_T and V_E were normalised for body mass (per 100 g).

2.4. Cardiorespiratory assessment under urethane anesthesia in wild-type and TgF344-AD rats

2.4.1. Surgical approach

Cardiorespiratory indices were assessed in WT (male n = 9; female n = 9) and TgF344-AD (male n = 7; female n = 12) animals under urethane anesthesia (1.5 g/kg I.P.; 20%w/v). The depth of anesthesia was monitored throughout the study by assessing reflex response to tail/paw pinch and the corneal reflex. Animals were placed in the supine position and core body temperature was maintained at 37 °C using a rectal temperature probe and homeothermic blanket system (Harvard Apparatus, Holliston, MA, USA). Once the relevant experimental protocols had been completed, the animals were euthanised by intravenous urethane overdose.

A mid-cervical tracheotomy was performed and the right jugular vein was cannulated for I.V. infusion of supplemental anesthetic and drugs. The right carotid artery was cannulated for recording of arterial blood pressure and withdrawal of arterial blood samples for blood gas and pH assessment. All animals were maintained with a bias flow of

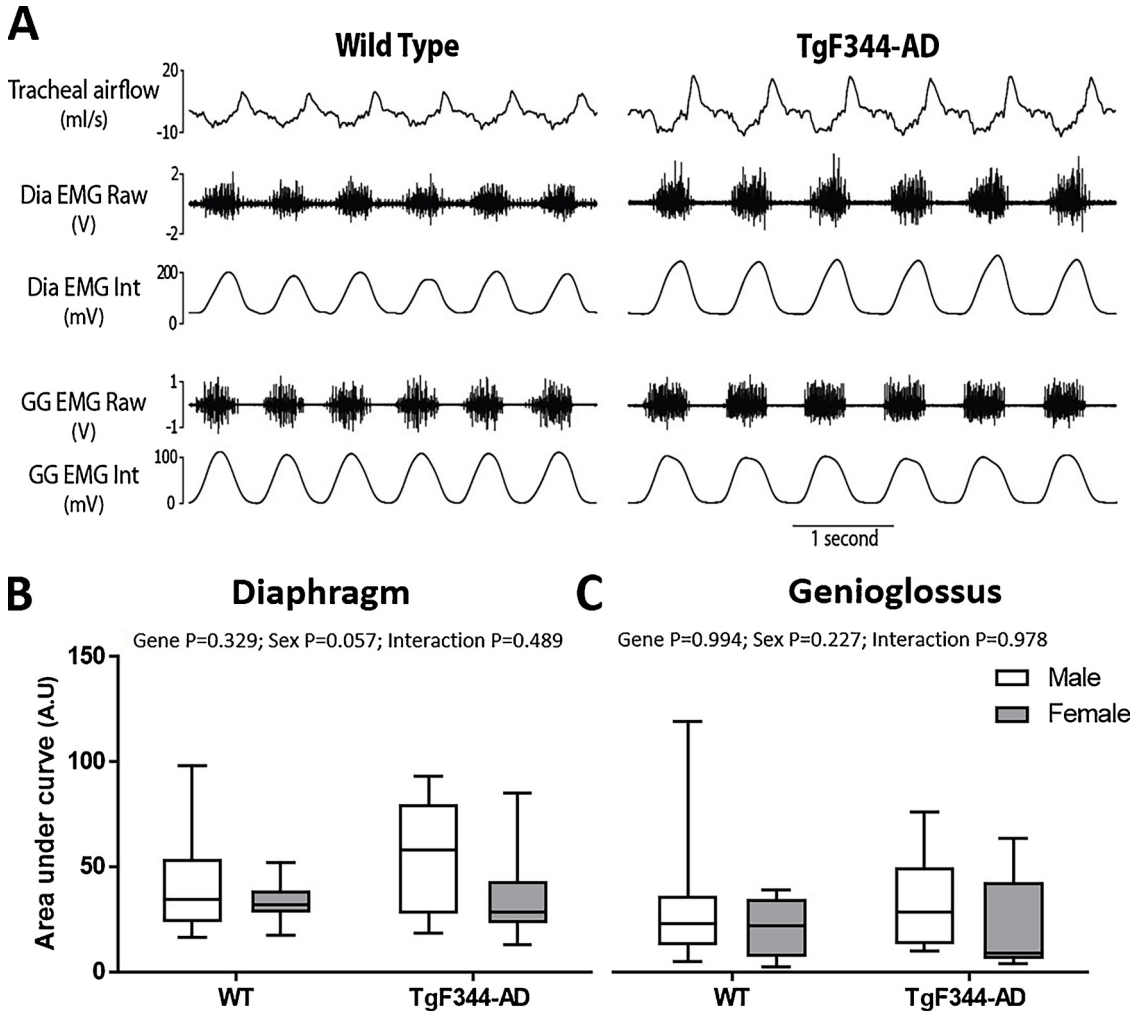

Fig. 3. Baseline Diaphragm and Genioglossus EMG Activity in Anesthetised Wild-Type and TgF344-AD Rats.
A) Representative traces of tracheal airflow, raw and integrated diaphragm (Dia) and genioglossus (GG) electromyogram (EMG) activity in wild-type and TgF344-AD rats. Group data for area under the curve analysis of integrated Dia (B) and integrated GG (C) EMG activity. Values (B and C) are expressed as box and whisker plots (median, 25–75 percentiles and minimum and maximum values). Dia, diaphragm; GG, genioglossus; WT, wild type. Groups were statistically compared by two-way ANOVA (gene x sex) with Bonferroni *post hoc* test.

supplemental O_2 to maintain arterial oxygen saturation (SaO_2) above 95% unless otherwise specified.

A pneumotachometer (Hans Rudolph Inc., KS, USA) was connected in series to the tracheal cannula to determine tracheal flow and a side arm was connected to a CO_2 analyser (microCapStar End-Tidal CO_2 analyser; CWE inc., USA) to determine end-tidal CO_2. Concentric needle electrodes (26 G; Natus Manufacturing Ltd, Ireland) were inserted into the costal diaphragm and genioglossus muscles for continuous measurement of diaphragm and genioglossus electromyogram (EMG) activity, respectively. The signals were amplified (x5,000), filtered (band pass; 500-5,000 Hz) and integrated (50 ms time constant; Neurolog system, Digitimer Ltd, UK). All data were digitised and displayed using LabChart (ADInstruments).

2.4.2. Experimental protocol

Following a 30-minute period of stabilisation, an arterial blood sample was acquired and baseline parameters were assessed over a 10-minute period. Once satisfied that parameters were steady-state we performed a series of experimental challenges. A minimum of 10 min recovery was afforded following each challenge to allow the return of stable parameter recordings between challenges. Airflow to the lungs was occluded for 10 attempted breaths via complete obstruction of the pneumotachometer. The 5-HT_3 agonist, phenylbiguanide (25 μg/kg) was administered intravenously to stimulate pulmonary vagal C-fibre afferent nerves thereby eliciting the pulmonary chemoreflex. A single male TgF344-AD rat was classified as a non-responder to phenylbiguanide stimulation as no apnoea or tachypnoea was elicited; therefore, the animal was excluded from group analysis.

A subset of animals were vagotomised via bilateral section of the cervical vagi. After a 20-minute recovery period, the bias airflow was manipulated to determine the cardiorespiratory reflex responses to chemostimulation. A graded hypercapnic challenge was performed whereby animals were challenged with increasing levels of inspired carbon dioxide: $FiCO_2 = 0.05$ and $FiCO_2 = 0.10$ (supplemental O_2; balance N_2) consecutively for five minutes each. Subsequent to recovery from the hypercapnic stimulus, animals were exposed to hypoxia ($FiO_2 = 0.12$, balance N_2) for five minutes. Finally, once recovered, rats were challenged with a five minute asphyxia stimulus ($FiO_2 = 0.12$, $FiCO_2 = 0.05$, balance N_2).

Following euthanasia, whole brains were immediately harvested. The pons and medulla oblongata regions were isolated and frozen in dry-ice cooled isopentane and stored at −80 °C until required.

2.4.3. Data analysis

Area under the curve (AUC) of integrated diaphragm and genioglossus EMG activity was analysed and averaged under steady-state

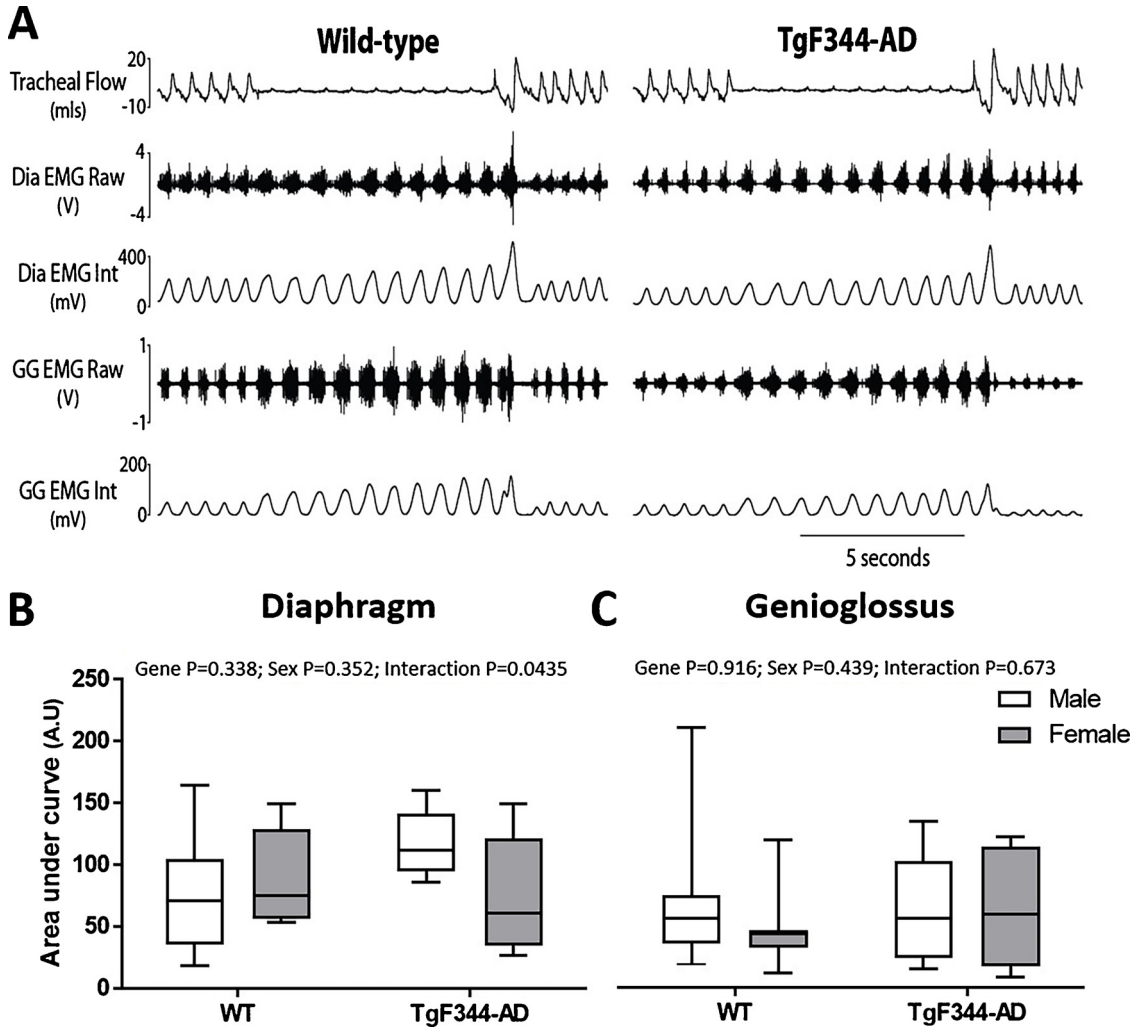

Fig. 4. Diaphragm and Genioglossus EMG Response to Tracheal Occlusion in Anesthetised Wild-Type and TgF344-AD Rats.
A) Representative traces of tracheal airflow, raw and integrated diaphragm (Dia) and genioglossus (GG) electromyogram (EMG) activity in wild-type and TgF344-AD rats during a ten-breath tracheal occlusion challenge. Group data (mean ± SD) for area under the curve analysis of integrated Dia (B) and GG (C) EMG activity). Dia, diaphragm; GG, genioglossus; WT, wild type. Data (B and C) are expressed as box and whisker plots (median, 25–75 percentiles and minimum and maximum values). Groups were statistically compared by two-way ANOVA (gene x sex) with Bonferroni *post hoc* test.

baseline conditions, and for 90 s of baseline (pre-challenge) immediately prior to obstructive, chemostimulation and drug challenges. All AUC diaphragm and genioglossus integrated EMG data are reported in arbitrary units. Maximum apnoea and post-apnoea tachypnoea data from phenylbiguanide stimulation were expressed as the duration of the apnoea/tachypnoea period normalised to the expiratory duration from the pre-challenge baseline value. AUC of diaphragm and genioglossus integrated EMG activity post-vagotomy was analysed over a ten-minute baseline period. During chemostimulation challenges, the average of the ten breaths surrounding the maximal response elicited during each challenge was expressed in arbitrary units.

2.5. Western immunoblot and pro-inflammatory multiplex assay of brain homogenates from wild-type and TgF344-AD rats

2.5.1. Tissue homogenisation

Tissue was weighed and homogenised at a concentration of 100 mg/mL in radioimmunoprecipitation assay (RIPA) lysis buffer, which consisted of 10 mM Tris-HCl (pH 8), 150 mM NaCl, 0.5% IGEPAL-CA630, 0.5% sodium deoxycholate, 0.1% SDS containing protease inhibitors (5 mM EDTA, 1 mM EGTA, 5ug/ml leupeptin, 5 µg/ml aprotinin, 2 µg/ml pepstatin, 120 µg/ml Pefabloc, 2 mM 1,10-phenanthroline). Samples were subsequently spun at 10,000 x g for 10 min at 4 °C, to pellet membranes and nuclei. Supernatants were diluted 1:10 with RIPA buffer and protein concentrations were determined using a bicinchoninic acid (BCA) assay (Thermo Fisher Scientific, USA). Cell lysates were equalised for protein concentration to 1 mg/mL before use in subsequent biochemical analyses.

2.5.2. Western blot

Cell lysates containing equivalent protein concentrations were mixed with the 5X SDS Laemmli buffer containing 5% β-mercaptoethanol, 0.02% bromophenol blue, 50% (v/v) sterile glycerol, 1% (w/v) SDS and 50 mM of Tris-HCl buffer (pH-6.8) and boiled for 5 min at 95 °C. Samples for the resolution of APP C-terminal fragments (CTF) were prepared by mixing equivalent protein concentrations with 4X Tris-Tricine sample buffer containing 40% (v/v) sterile glycerol, 16% (w/v) SDS, 50 mM of Tris-HCl buffer (pH-8.45) and 0.04% phenol red and boiled for 5 min at 95 °C. Proteins were resolved on 10% or 16% Tris-glycine/Tricine SDS-PAGE gels depending on the protein of interest. Proteins were then transferred onto 0.2µM pore size nitrocellulose membrane (Amersham, USA). Membranes were then blocked in 5% (w/v) reconstituted skimmed milk (Marvel) in TBS-Tween-20 (0.1%) for 1 h and then incubated with primary antibody

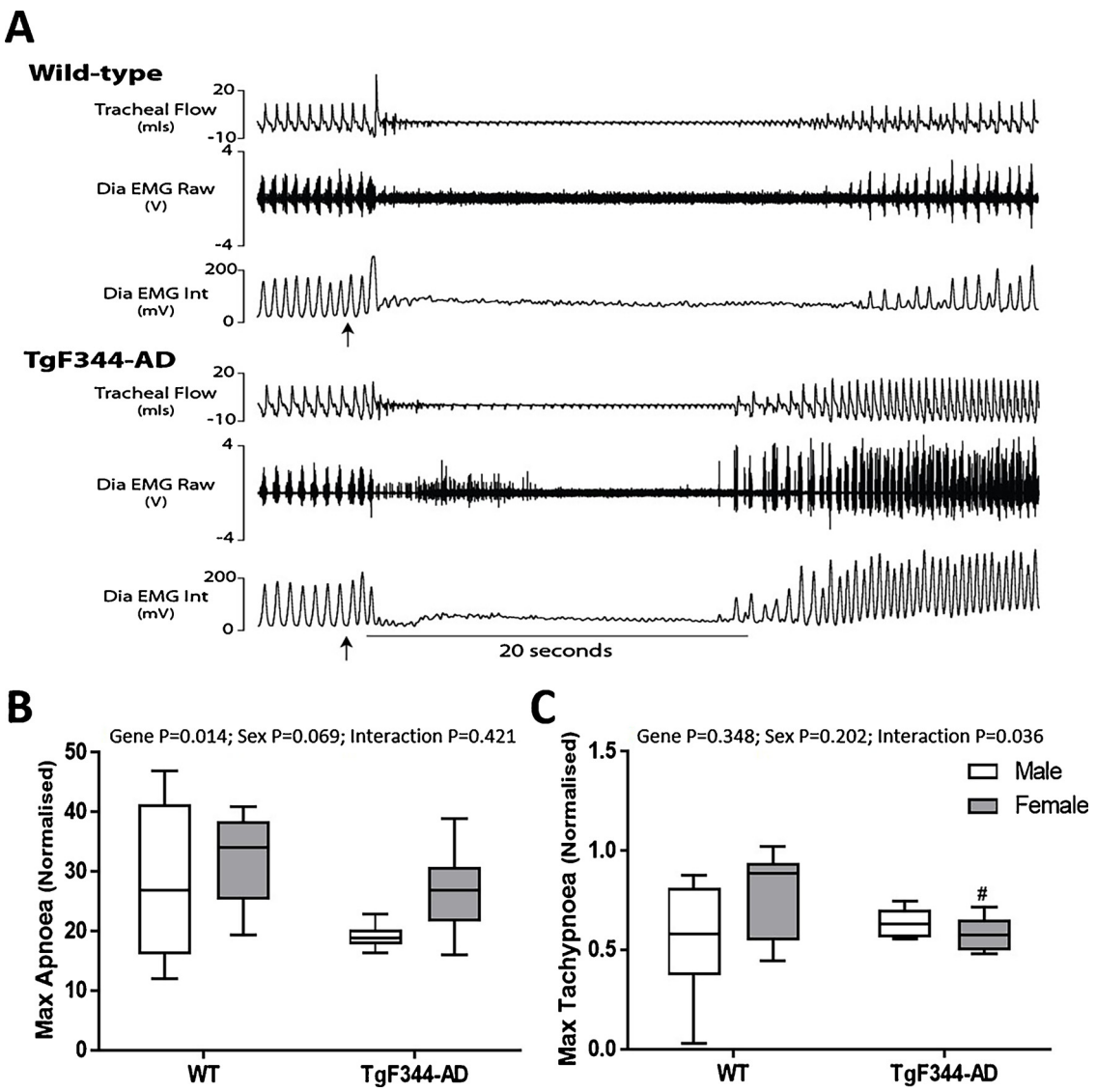

Fig. 5. Pulmonary Chemoreflex Response to i.v. Phenylbiguanide in Anesthetised Wild-Type and TgF344-AD Rats.
A) Representative traces of tracheal airflow, raw and integrated diaphragm (Dia) electromyogram (EMG) activity in wild-type and TgF344-AD rats during i.v. administration of phenylbiguanide (25 μg/kg) indicated by the upwards arrow. Group data for two key components of the pulmonary chemoreflex response: maximum apnoea duration (B) and maximum tachypnoea (C) normalised to baseline respiratory period. WT, wild type. Data (B and C) are expressed as box and whisker plots (median, 25–75 percentiles and minimum and maximum values; WT (male n = 9; female n = 9) and TgF344-AD (male n = 6; female n = 12)). Groups were statistically compared by two-way ANOVA (gene x sex) with Bonferroni *post hoc* test. *WT female versus WT male, $p < 0.05$. # TgF344-AD female versus WT female, $p < 0.05$.

(1:1000 dilution) overnight at 4 °C on a roller. Following primary antibody incubation, the blots were incubated for one hour with secondary antibody conjugated to horse-radish peroxidase enzyme (1:5000 dilution). Blots were then washed three times in TBS-T (0.1%), ten minutes per wash, and analysed using an enhanced chemiluminescence reagent (Pierce), with respective protein bands being obtained by exposure of membranes to X-ray film. Tubulin was used as a loading control ensuring equal protein content in each well.

2.5.3. Pro-inflammatory cytokine multiplex assay

Levels of interferon (IFN)-γ, IL-1β, IL-4, IL-5, IL-10, IL-13, keratinocyte chemoattractant/growth-related oncogene (KC/GRO) and TNF-α were measured in pons and medulla oblongata supernatants by sandwich immunoassay methods using commercially available detection kits (V-Plex Pro-inflammatory Panel 2 (rat) kit; Meso Scale Discovery, Gaithersburg, USA) as per manufacturer's instructions. 100 μg of protein sample was loaded per well with all samples analysed in duplicate and compared with known concentrations of protein standards. Plates were analysed using a QuickPlex SQ 120 plate reader (Meso Scale Discovery).

2.6. Statistical analysis

Values are expressed as mean ± SD or displayed graphically as box and whisker plots. Data were statistically analysed using Prism 5.0 (Graphpad Software, CA, USA). All data were statistically compared by two-way ANOVA with Bonferroni *post hoc* test or by repeated measures two-way ANOVA. $p < 0.05$ was considered statistically significant in all tests.

Table 3
Baseline Cardiorespiratory Parameters in Anesthetised Vagotomised Wild-Type and TgF344-AD Rats.

	Wild-type		TgF344-AD		
	Male (n = 8)	Female (n = 8)	Male (n = 6)	Female (n = 10)	Two-way ANOVA
f_R (bpm)	50 ± 7	49 ± 3	49 ± 4	48 ± 7	Gene: p = 0.763 Sex: p = 0.8; Interaction: p = 0.951
V_T (ml/100 g)	1.77 ± 0.38	1.30 ± 0.19	1.98 ± 0.29	1.63 ± 0.29	Gene: p = 0.019; Sex: p < 0.001; Interaction: p = 0.525
V_E (ml/min/100 g)	89.2 ± 32.0	63.5 ± 8.6	97.42 ± 22.1	79.8 ± 22.9	Gene: p = 0.1486; Sex: p = 0.014; Interaction: p = 0.63
MAP (mmHg)	90.0 ± 7.5	93.6 ± 5.5	92.0 ± 9.9	94.6 ± 12.1	Gene: p = 0.66 Sex: p = 0.358; Interaction: p = 0.898
HR (bpm)	446 ± 22	455 ± 5.9	475 ± 73	400 ± 123	Gene: p = 0.143; Sex: p = 0.243; Interaction: p = 0.143
PO_2 (mmHg)	99 ± 14	99 ± 7	104 ± 17	117 ± 18	Gene: p = 0.057; Sex: p = 0.282; Interaction: p = 0.293
PCO_2 (mmHg)	47.4 ± 3.4	49.7 ± 4.4	49.4 ± 2.8	44.0 ± 6.8	Gene: p = 0.338; Sex: p = 0.416; Interaction: p = 0.05
pH	7.36 ± 0.03	7.35 ± 0.03	7.35 ± 0.02	7.40 ± 0.07	Gene: p = 0.255; Sex: p = 0.281; Interaction: p = 0.118
HCO_3^- (mmol/l)	26.8 ± 1.2	27.0 ± 1.5	26.6 ± 0.9	25.3 ± 1.9	Gene: p = 0.139; Sex: p = 0.36; Interaction: p = 0.204
Haematocrit (%)	47.9 ± 3.7	49.7 ± 1.0	48.8 ± 2.6	47.2 ± 2.0	Gene: p = 0.44; Sex: p = 0.927; Interaction: p = 0.082
Haemoglobin (g/dl)	16.3 ± 1.3	16.9 ± 0.3	16.6 ± 0.9	16.0 ± 0.7	Gene: p = 0.388; Sex: p = 0.96; Interaction: p = 0.071

f_R, respiratory frequency; V_T, tidal volume; V_E, minute ventilation; MAP, mean arterial pressure; HR, heart rate; PO_2, partial pressure of oxygen; PCO_2, partial pressure of carbon dioxide; HCO_3^-, bicarbonate. Data are shown as mean ± SD and were statistically compared by two-way ANOVA (gene x sex) with Bonferroni *post hoc* test.

Table 4
Baseline Diaphragm and Genioglossus EMG Activity in Anesthetised Vagotomised Wild-Type and TgF344-AD Rats.

	Wild-type		TgF344-AD		
	Male (n = 8)	Female (n = 8)	Male (n = 6)	Female (n = 10)	Two-way ANOVA
Diaphragm AUC (arbitrary units)	59 ± 42	67 ± 33	97 ± 34	74 ± 43	Gene: p = 0.122; Sex: p = 0.615; Interaction: p = 0.267
Genioglossus AUC (arbitrary units)	136 ± 104	117 ± 59	82 ± 60	71 ± 42	Gene: p = 0.054; Sex: p = 0.546; Interaction: p = 0.872

AUC, area under the curve. Data are shown as mean ± SD and were statistically compared by two-way ANOVA (gene x sex) with Bonferroni *post hoc* test.

3. Results

3.1. Baseline ventilation and ventilatory responses to chemostimulation in conscious wild-type and TgF344-AD rats

Baseline minute ventilation normalised to body mass was significantly lower in males compared with females (Table 1), owing to significantly heavier male body weights and the ontogenetic scaling differences of the lungs between sexes (Stewart and German, 1999). Respiratory rate was significantly higher in TgF344-AD males compared with TgF344-AD females. Male rats tended to have a higher sigh count (Fig. 1B) and apnoea index (Fig. 1C) compared with females; apnoea durations were equivalent (Fig. 1D). Ventilation and respiratory behaviour was equivalent in WT and TgF344-AD rats. The hypoxic ventilatory response was equivalent in WT and TgF344-AD rats for both sexes (Fig. 2B and C). The ventilatory response to hypercapnia tended to be less in male TgF344-AD rats compared with WT (Fig. 2B), whereas the response in female TgF344-AD and WT rats was equivalent (Fig. 2C).

3.2. Cardiorespiratory and haematological parameters in anesthetised wild-type and TgF344-AD rats

There were no significant differences for baseline cardiorespiratory parameters between anesthetised WT and TgF344-AD rats. Haematocrit was lower in TgF344-AD rats compared with WT (Table 2), however no significant difference between groups was detected by Bonferroni *post-hoc* analysis.

3.3. Respiratory muscle EMG activity in wild-type and TgF344-AD rats

Baseline diaphragm (Fig. 3B) and genioglossus (Fig. 3C) EMG activity was equivalent in WT and TgF344-AD rats. Diaphragm EMG (Fig. 4B) and genioglossus EMG (Fig. 4C) responses to tracheal airway occlusion were similar between all groups. Vagal afferent stimulation by phenylbiguanide produced significantly shorter apnoea durations in TgF344-AD rats compared with WT (p = 0.014; Fig. 5B), although *post hoc* analysis revealed no significant differences. The tachypnoeic episode of the evoked pulmonary chemoreflex was significant in magnitude in WT females compared with WT males and blunted in TgF344-AD female rats compared with WT female rats (Fig. 5C).

3.4. Cardiorespiratory responses to chemostimulation in anesthetised vagotomised wild-type and TgF344-AD rats

Following bilateral cervical vagotomy, cardiorespiratory parameters were similar in WT and TgF344-AD rats (Table 3). TgF344-AD rats tended to have blunted genioglossus EMG activity during baseline

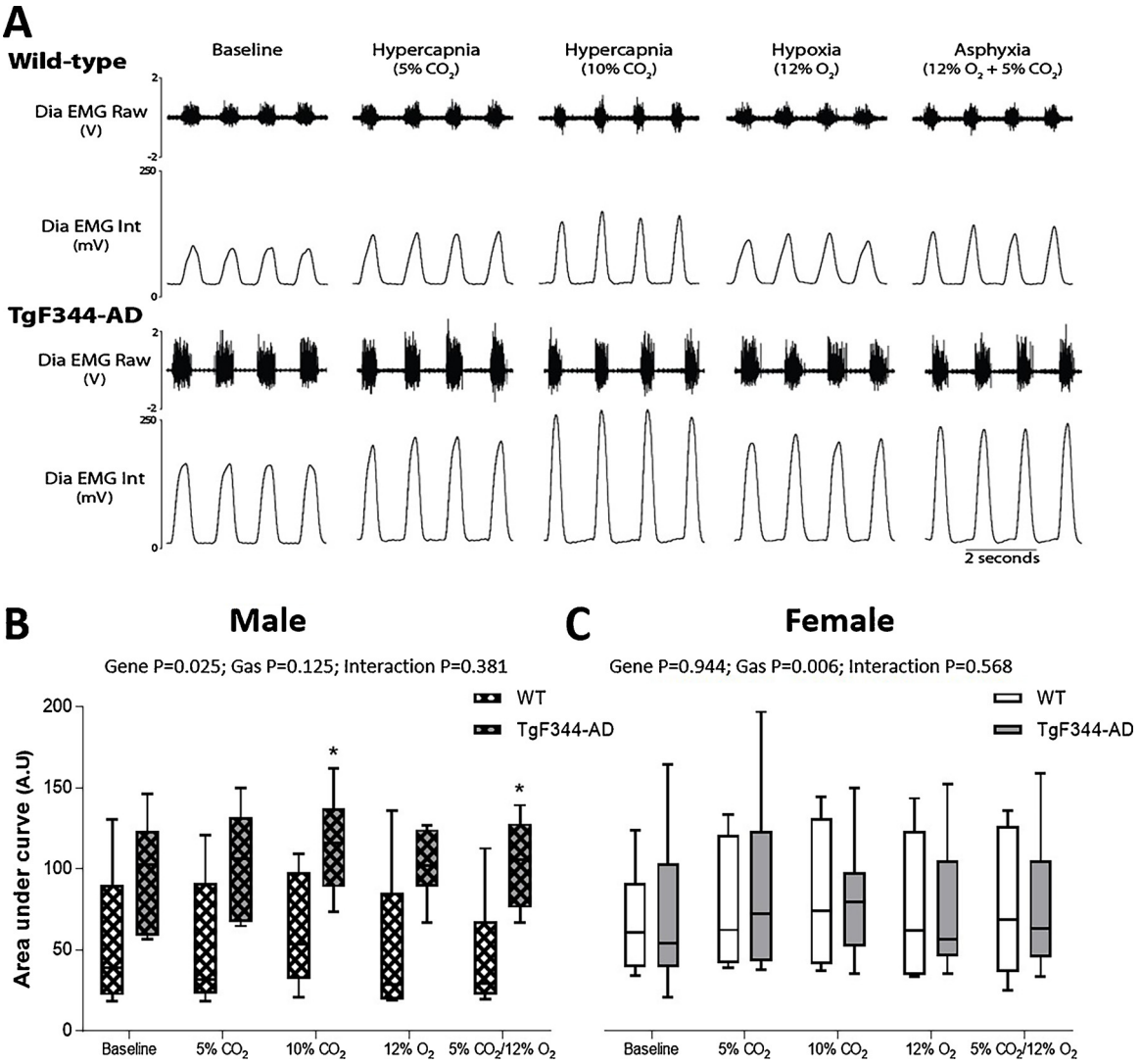

Fig. 6. Diaphragm EMG Responses to Chemostimulation in Anesthetised Vagotomised Wild-Type and TgF344-AD Rats.
A) Representative traces of raw and integrated diaphragm (Dia) electromyogram (EMG) activity in wild-type and TgF344-AD rats during baseline, hypercapnic, hypoxic and asphyxic breathing. Group data for area under the curve analysis of integrated Dia EMG activity in males (B; WT n = 7, TgF344-AD n = 6) and females (C; WT n = 8, TgF344-AD n = 8) in response to chemostimulation. Dia, diaphragm; WT, wild type. Data (B and C) are expressed as box and whisker plots (median, 25–75 percentiles and minimum and maximum values). Groups were statistically compared by repeated measures two-way ANOVA (gene x gas) with Bonferroni *post hoc* test. * WT versus TgF344-AD, $p < 0.05$.

compared with WT rats (Table 4). Diaphragm EMG activity was significantly greater in male TgF344-AD rats compared with male WT ($p = 0.025$, Fig. 6B); *post hoc* analysis revealed significantly increased diaphragm EMG activity both in response to hypercapnic and asphyxic chemostimulation ($p < 0.05$). Interestingly, diaphragm EMG activity in female TgF344-AD rats was similar to female WT rats throughout all chemostimulation challenges (Fig. 6C). Genioglossus EMG activity was equivalent in WT and TgF344-AD male rats (Fig. 7B), and in female rats (Fig. 7C) across all gas challenges.

3.5. APP metabolism and Tau protein phosphorylation in brainstem from wild-type and TgF344-AD rats

The expression of full length APP and APP-CTFs were significantly increased in the brainstem of TgF344-AD rats compared with WT rats ($p < 0.001$, Fig. 8D). Interestingly, the ratio of β-CTFs to α-CTFs was significantly increased in TgF344-AD rats compared with WT rats ($p < 0.001$), both in the pons and medulla oblongata. The expression of β-CTFs relative to α-CTFs was significantly higher in the medulla oblongata compared with the pontine region ($p < 0.05$) in WT and TgF344-AD rats. Tau phosphorylation was not significantly altered in the pontine or medulla oblongata brainstem regions in TgF344-AD rats compared with WT rats (Fig. 8E). Aβ levels were below the limit of immunoblot detection, suggesting minimal Aβ deposition in the TgF344-AD rat brainstem at this age (8–11 months).

3.6. Cytokine concentrations in brainstem from wild-type and TgF344-AD rats

The concentrations of pro-inflammatory cytokines were equivalent in WT and TgF344-AD pons and medulla oblongata samples (Table 5).

4. Discussion

AD is notoriously difficult to detect before irreversible damage has developed in the central nervous system. The purpose of this study was to determine if aberrant respiratory control develops as a prodromal feature, prior to the emergence of overt cognitive dysfunction in a novel animal model of the disease, the TgF344-AD rat. At age 8–11 months, no profound aberrant cardiorespiratory pathophysiology was detected

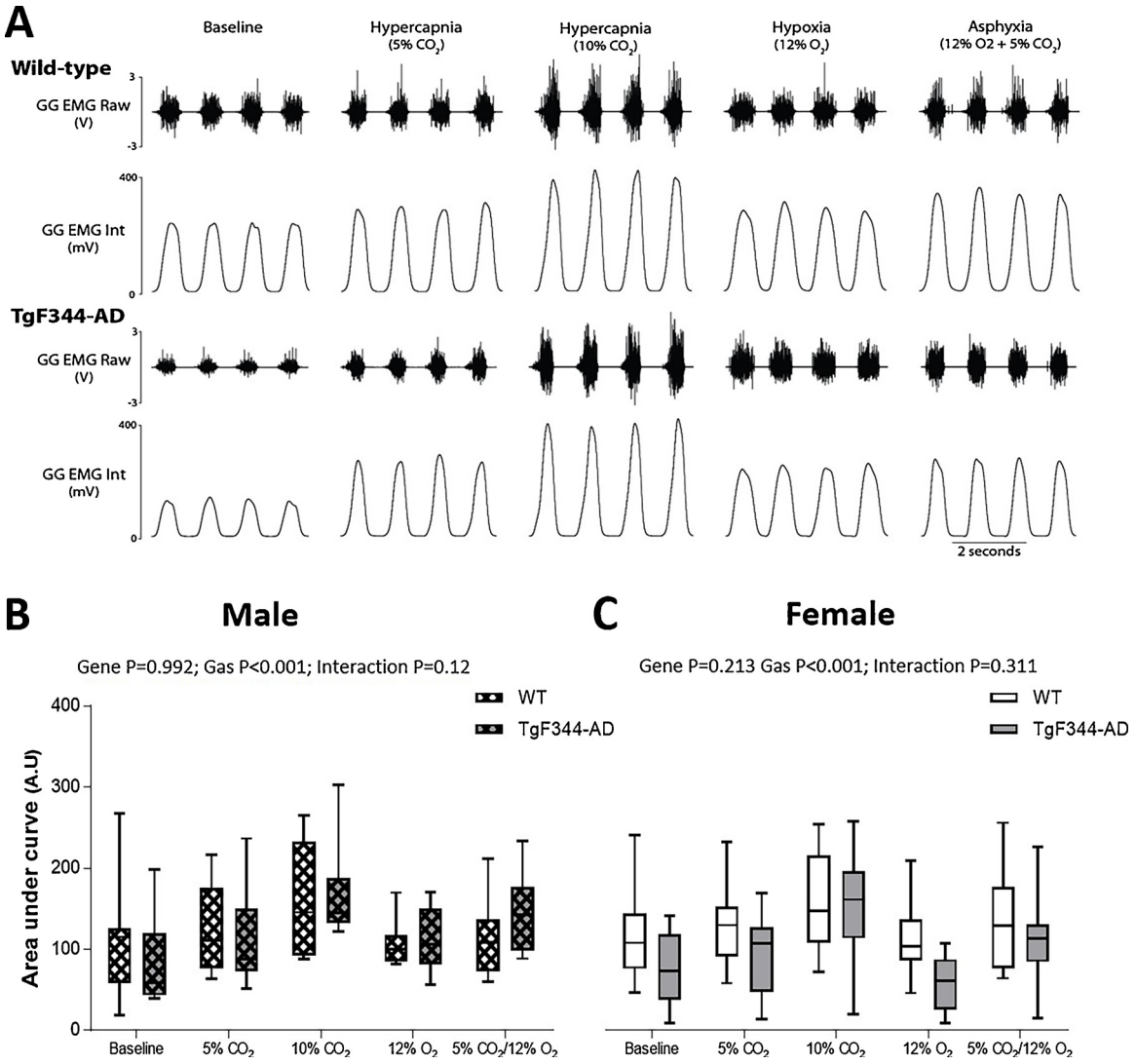

Fig. 7. Genioglossus EMG Responses to Chemostimulation in Anesthetised Vagotomised Wild-Type and TgF344-AD Rats.
A) Representative traces of raw and integrated genioglossus (GG) electromyogram (EMG) activity in wild-type and TgF344-AD rats during baseline, hypercapnic, hypoxic and asphyxic breathing. Group data for area under the curve analysis of integrated GG EMG activity in males (B; WT n = 7, TgF344-AD n = 6) and females (C; WT n = 8, TgF344-AD n = 8) in response to chemostimulation. GG, genioglossus; WT, wild type. Data (B and C) are expressed as box and whisker plots (median, 25–75 percentiles and minimum and maximum values). Groups were statistically compared by repeated measures two-way ANOVA (gene x gas) with Bonferroni *post hoc* test.

in transgenic rats, such that we observed normal breathing and ventilatory responsiveness, and no indications of brainstem tau hyperphosphorylation, Aβ deposition, or neuroinflammation despite evidence of altered APP metabolism (increased C-terminal fragments) in the pons and medulla oblongata of transgenic animals. Subtle sex-specific alterations to central chemosensitivity and blunted apnoea duration in response to noxious vagal afferent nerve stimulation were observed in TgF344-AD rats, however we consider these insubstantial in the pursuit of a robust AD-related aberrant respiratory prodromal, or overt pathological, signature.

Upper airway dysfunction is a characteristic feature in AD (Boccardi et al., 2016). Whilst subtle respiratory system remodelling was evident in transgenic animals in our study, upper airway motor function, as determined from genioglossus EMG recordings, was well maintained in TgF344-AD rats at 8–11 months of age. The trend towards blunted hypercapnic ventilatory responsiveness in conscious male TgF344-AD rats may reflect the emergence of atypical central chemosensitivity. Of note, elevated diaphragm responsiveness during hypercapnic chemostimulation was observed in the vagotomised anesthetised male TgF344-AD rats compared with WT, suggesting that subtle changes in respiratory control in male TgF344-AD rats are state-dependent. However, it is evident from our study considering all data, that respiratory control is very well preserved in this AD rat model. Beyond the broad assessment of cardiorespiratory physiological function, we measured medullary and pontine cytokine levels, which revealed that there were no significant differences between wild-type and TgF344-AD rats, and no evidence of neuroinflammation in the AD brainstem at this stage of disease progression. It is conceivable that altered APP metabolism could be responsible for subtle respiratory responses reported herein prior to the potential emergence of neuroinflammation at a later stage. In a rodent model of AD that overexpresses mutant APP and PS1, Liu et al. (2008) reported no increase in hyperphosphorylated tau protein, similar to the findings in the present study. The increased ratio of β-:α-CTFs confirms the preferential cleavage of APP by β-secretase associated with the Swedish mutation of APP (Citron et al., 1992). We hypothesise that whilst an elevated abundance of noxious β-CTFs are evidently expressed within brainstem neurons of the TgF344-AD rat, the absence of neuroinflammation, paralleled with a largely

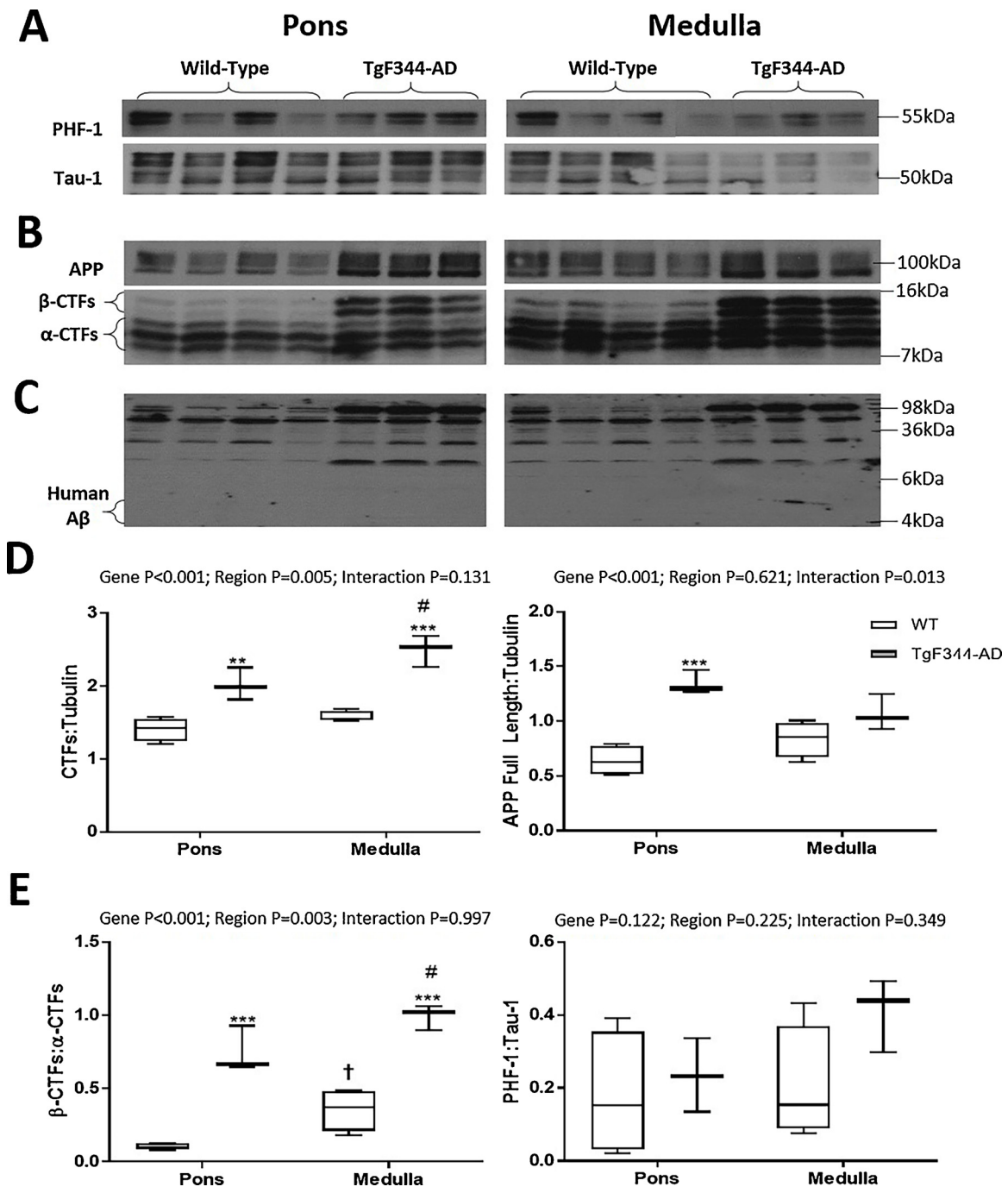

Fig. 8. Western Blot Detection of Tau and APP Derivatives in Wild-Type and TgF344-AD Rat Brainstem Homogenates.
Western blot gels of (A) phosphorylated tau at serine sites 396/404 (top) and dephosphorylated tau at serine sites 195/202 (bottom), (B) full length APP (top) as well as α-CTF and β-CTFs (bottom). Blots for detection of human Aβ were negative in all wild-type and TgF344-AD samples (C). Group data (WT n = 4; TgF344-AD, n = 3) for CTF and APP concentration normalised to tubulin (D) as well as the expression of β-CTFs relative to α-CTFs and the ratio of phosphorylated tau relative to unphosphorylated tau (E). Aβ, amyloid-β; APP, amyloid precursor protein; CTFs, C-terminal fragments; WT, wild type. Data (D–E) are expressed as box and whisker plots (median, 25–75 percentiles and minimum and maximum values). Groups were statistically compared by two-way ANOVA (gene x brainstem region) with Bonferroni *post hoc* test. ** WT versus TgF344-AD, $p < 0.01$ *** WT versus TgF344-AD, $p < 0.001$; † WT medulla versus WT pons, $p < 0.05$; # TgF344-AD medulla versus TgF344-AD pons.

undisturbed respiratory phenotype, suggests that brainstem neurological function is unimpaired at this stage of disease progression in this model. Although tau hyperphosphorylation has been observed in cerebral regions of TgF344-AD rats, this phenotype may be dependent upon the age of the animal and the method used to isolate protein samples (Cohen et al., 2013). Of note, neuroinflammation is prevalent in several animal models of AD such as the 3xTg mouse (Magistri et al., 2016), 5xFAD mouse (Gurel et al., 2018), TgCRND8 mouse (Djordjevic et al., 2017), amyloid-β1–42 mouse (Souza et al., 2018), and the streptozotocin rat (Mishra et al., 2017), and this observation extends to the TgF344-AD rat (Cohen et al., 2013) used in the present study. It is also important to recognise that respiratory deficits have been described in AD animal models (Dutschmann et al., 2010; Menuet et al., 2011a), but were not evident using our experimental approach in

Table 5
Cytokine Concentrations in Pons and Medulla of Wild-Type and TgF344-AD Rats.

	Pons		Medulla		
(pg/mg protein)	WT (n = 11)	TgF344-AD (n = 8)	WT (n = 11)	TgF344-AD (n = 8)	Two-way ANOVA
IFN-y	7.94 ± 1.19	7.69 ± 0.56	7.81 ± 1.01	7.96 ± 1.17	Gene: p = 0.887; Region: p = 0.846; Interaction: p = 0.567
IL-1β	12.91 ± 2.39	14.01 ± 1.91	14.45 ± 3.82	14.95 ± 4.18	Gene: p = 0.453; Region: p = 0.247; Interaction: p = 0.778
IL-4	0.329 ± 0.028	0.333 ± 0.036	0.343 ± 0.032	0.367 ± 0.040	Gene: p = 0.22; Region: p = 0.036; Interaction: p = 0.39
IL-5	10.18 ± 1.18	11.03 ± 0.88	10.64 ± 1.64	11.36 ± 1.98	Gene: p = 0.118; Region: p = 0.421; Interaction: p = 0.894
IL-10	19.92 ± 2.37	19.90 ± 2.01	20.54 ± 2.27	20.91 ± 2.85	Gene: p = 0.828; Region: p = 0.305; Interaction: p = 0.804
IL-13	0.824 ± 0.023	0.825 ± 0.017	0.855 ± 0.054	0.885 ± 0.033	Gene: p = 0.255; Region: p = 0.002; Interaction: p = 0.282
KC/GRO	10.61 ± 2.25	10.57 ± 1.64	12.92 ± 4.60	14.92 ± 4.35	Gene: p = 0.507; Region: p = 0.032; Interaction: p = 0.491
TNF-α	0.395 ± 0.044	0.392 ± 0.042	0.438 ± 0.060	0.449 ± 0.062	Gene: p = 0.815; Region: p = 0.006; Interaction: p = 0.668

IFN-y, interferon-y; IL-1β, interleukin-1β; IL-4, interleukin-4; IL-5, interleukin-5; IL-10, interleukin-10; IL-13, interleukin-13; KC/GRO, keratinocyte chemoattractant/growth-related oncogene; TNF-α, tumour necrosis factor. Data are shown as mean ± SD and were statistically compared by two-way ANOVA (gene x brainstem region) with Bonferroni *post hoc* test.

TgF344-AD rats at 8–11 months.

In addition to our assessment of ventilation and ventilatory responsiveness to chemostimulation, we also explored other important aspects of respiratory behaviour providing a broad screening of the respiratory phenotype in TgF344-AD rats. In particular, we focussed on apnoeas and augmented breaths in the expectation that aberrant central neural network activity would manifest in overt alterations in these parameters. However, as there were no appreciable differences in the incidence of sighs and apnoeas between WT and TgF344-AD animals, we conclude that central respiratory network function is unimpaired, at least at our level of detection. However, reduced apnoea duration in TgF344-AD rats in response to noxious vagal afferent nerve stimulation with phenylbiguanide revealed a blunted pulmonary chemoreflex, which may reflect altered central processing of vagal afferent control of breathing. Serotonin (5-HT) plays an influential role in modulating central chemosensitivity as well as the ventilatory behaviours described above (Iceman et al., 2013; Teran et al., 2014). Altered 5-HT metabolism is reported in an 8-month old model of AD (Tau.P301L mice) (Menuet et al., 2011a). If this is reflected in the TgF344-AD rat model it may translate to an emergent altered reflex control of breathing, which we speculate develops more robustly in TgF344-AD rats later in the disease.

In summary, we report that respiratory control is well maintained in 8–11 month old TgF344-AD rats, with no evidence of tau hyperphosphorylation, Aβ accumulation or neuroinflammation in the brainstem. Notwithstanding suggestions that brainstem neurodegeneration may be a precursor to the development of overt AD, it is evident in our study that either insufficient, or completely absent, brainstem neurological deterioration developed in the TgF344-AD rat by 8–11 months of age. Of note, at six months of age, neuronal loss and apoptosis are not evident in the cerebrum of this animal model, however the animals do present with neuroinflammation and Aβ deposition as well as an abundance of soluble Aβ1-40 (Cohen et al., 2013). We observed that the brainstem region of this animal model displays altered APP metabolism (increased abundance if toxic β-C-terminal fragments), but is otherwise unaffected at this stage of the disease. We acknowledge that cognitive deficits were not assessed in this animal model at 8–11 months, thus no behavioural markers of disease progression are presented. Based on the study by Cohen et al. (2013) we suspect that in TgF344-AD rats at 24 months of age, which present with severe learning and memory deficiency, respiratory function may become dysregulated through loss of neuronal function in brainstem regions. However, our study provides no evidence in support of a prodromal respiratory control signature in theTgF344-AD rat model.

Conflicts of interest

None.

Funding and acknowledgements

This study was funded by the Department of Physiology, University College Cork and Strategic Research Funding from University College Cork to MGR and KDO'H. We are grateful to staff of the Biological Services Unit, University College Cork for their support in the breeding and maintenance of rat colonies. We are grateful to Prof. Terrence Town and Dr. Tara M. Weitz for providing us with the TgF344-AD rat model.

References

Akiyama, H., Barger, S., Barnum, S., Bradt, B., Bauer, J., Cole, G.M., Cooper, N.R., Eikelenboom, P., Emmerling, M., Fiebich, B.L., Finch, C.E., Frautschy, S., Griffin, W.S., Hampel, H., Hull, M., Landreth, G., Lue, L., Mrak, R., Mackenzie, I.R., McGeer, P.L., O'Banion, M.K., Pachter, J., Pasinetti, G., Plata-Salaman, C., Rogers, J., Rydel, R., Shen, Y., Streit, W., Strohmeyer, R., Tooyoma, I., Van Muiswinkel, F.L., Veerhuis, R., Walker, D., Webster, S., Wegrzyniak, B., Wenk, G., Wyss-Coray, T., 2000. Inflammation and Alzheimer's disease. Neurobiol. Aging 21, 383–421.

Boccardi, V., Ruggiero, C., Patriti, A., Marano, L., 2016. Diagnostic assessment and management of dysphagia in patients with Alzheimer's disease. J. Alzheimers Dis. 50, 947–955.

Borel, J.C., Melo-Silva, C.A., Gakwaya, S., Rousseau, E., Series, F., 2016. Diaphragm and genioglossus corticomotor excitability in patients with obstructive sleep apnea and control subjects. J. Sleep Res. 25, 23–30.

Borke, R.C., Nau, M.E., Ringler Jr, R.L., 1983. Brain stem afferents of hypoglossal neurons in the rat. Brain Res. 269, 47–55.

Citron, M., Oltersdorf, T., Haass, C., McConlogue, L., Hung, A.Y., Seubert, P., Vigo-Pelfrey, C., Lieberburg, I., Selkoe, D.J., 1992. Mutation of the beta-amyloid precursor protein in familial Alzheimer's disease increases beta-protein production. Nature 360, 672–674.

Cohen, R.M., Rezai-Zadeh, K., Weitz, T.M., Rentsendorj, A., Gate, D., Spivak, I., Bholat, Y., Vasilevko, V., Glabe, C.G., Breunig, J.J., Rakic, P., Davtyan, H., Agadjanyan, M.G., Kepe, V., Barrio, J.R., Bannykh, S., Szekely, C.A., Pechnick, R.N., Town, T., 2013. A transgenic Alzheimer rat with plaques, tau pathology, behavioral impairment, oligomeric abeta, and frank neuronal loss. J. Neurosci. 33, 6245–6256.

Daulatzai, M.A., 2013. Death by a thousand cuts in Alzheimer's disease: hypoxia–the prodrome. Neurotox. Res. 24, 216–243.

Djordjevic, J., Thomson, E., Chowdhury, S.R., Snow, W.M., Perez, C., Wong, T.P., Fernyhough, P., Albensi, B.C., 2017. Brain region- and sex-specific alterations in

mitochondrial function and NF-kappaB signaling in the TgCRND8 mouse model of Alzheimer's disease. Neuroscience 361, 81–92.
Dutschmann, M., Menuet, C., Stettner, G.M., Gestreau, C., Borghgraef, P., Devijver, H., Gielis, L., Hilaire, G., Van Leuven, F., 2010. Upper airway dysfunction of Tau-P301L mice correlates with Tauopathy in midbrain and ponto-medullary brainstem nuclei. J. Neurosci. 30, 1810–1821.
Emamian, F., Khazaie, H., Tahmasian, M., Leschziner, G.D., Morrell, M.J., Hsiung, G.Y., Rosenzweig, I., Sepehry, A.A., 2016. The association between obstructive sleep apnea and Alzheimer's disease: a meta-analysis perspective. Front. Aging Neurosci. 8, 78.
Gurel, B., Cansev, M., Sevinc, C., Kelestemur, S., Ocalan, B., Cakir, A., Aydin, S., Kahveci, N., Ozansoy, M., Taskapilioglu, O., Ulus, I.H., Basar, M.K., Sahin, B., Tuzuner, M.B., Baykal, A.T., 2018. Early stage alterations in CA1 extracellular region proteins indicate dysregulation of IL6 and iron homeostasis in the 5XFAD Alzheimer's disease mouse model. J. Alzheimers Dis. 61, 1399–1410.
Heneka, M.T., Carson, M.J., Khoury, J.E., Landreth, G.E., Brosseron, F., Feinstein, D.L., Jacobs, A.H., Wyss-Coray, T., Vitorica, J., Ransohoff, R.M., Herrup, K., Frautschy, S.A., Finsen, B., Brown, G.C., Verkhratsky, A., Yamanaka, K., Koistinaho, J., Latz, E., Halle, A., Petzold, G.C., Town, T., Morgan, D., Shinohara, M.L., Perry, V.H., Holmes, C., Bazan, N.G., Brooks, D.J., Hunot, S., Joseph, B., Deigendesch, N., Garaschuk, O., Boddeke, E., Dinarello, C.A., Breitner, J.C., Cole, G.M., Golenbock, D.T., Kummer, M.P., 2015. Neuroinflammation in Alzheimer's disease. Lancet Neurol. 14, 388–405.
Iceman, K.E., Richerson, G.B., Harris, M.B., 2013. Medullary serotonin neurons are CO2 sensitive in situ. J. Neurophysiol. 110, 2536–2544.
Kokras, N., Stamouli, E., Sotiropoulos, I., Katirtzoglou, E.A., Siarkos, K.T., Dalagiorgou, G., Alexandraki, K.I., Coulocheri, S., Piperi, C., Politis, A.M., 2018. Acetyl cholinesterase inhibitors and cell-derived peripheral inflammatory cytokines in early stages of Alzheimer's disease. J. Clin. Psychopharmacol.
Liu, L., Orozco, I.J., Planel, E., Wen, Y., Bretteville, A., Krishnamurthy, P., Wang, L., Herman, M., Figueroa, H., Yu, W.H., Arancio, O., Duff, K., 2008. A transgenic rat that develops Alzheimer's disease-like amyloid pathology, deficits in synaptic plasticity and cognitive impairment. Neurobiol. Dis. 31, 46–57.
Lucking, E.F., O'Halloran, K.D., Jones, J.F., 2014. Increased cardiac output contributes to the development of chronic intermittent hypoxia-induced hypertension. Exp. Physiol. 99, 1312–1324.
Lue, L.F., Rydel, R., Brigham, E.F., Yang, L.B., Hampel, H., Murphy Jr, G.M., Brachova, L., Yan, S.D., Walker, D.G., Shen, Y., Rogers, J., 2001. Inflammatory repertoire of Alzheimer's disease and nondemented elderly microglia in vitro. Glia 35, 72–79.
Magistri, M., Velmeshev, D., Makhmutova, M., Patel, P., Sartor, G.C., Volmar, C.H., Wahlestedt, C., Faghihi, M.A., 2016. The BET-bromodomain inhibitor JQ1 reduces inflammation and tau phosphorylation at Ser396 in the brain of the 3xTg model of Alzheimer's disease. Curr. Alzheimer Res. 13, 985–995.
Manabe, T., Mizukami, K., Akatsu, H., Hashizume, Y., Ohkubo, T., Kudo, K., Hizawa, N., 2017. Factors associated with pneumonia-caused death in older adults with autopsy-confirmed dementia. Intern. Med. 56, 907–914.
Marin, J.M., Carrizo, S.J., Vicente, E., Agusti, A.G.N., 2005. Long-term cardiovascular outcomes in men with obstructive sleep apnoea-hypopnoea with or without treatment with continuous positive airway pressure: an observational study. Lancet 365, 1046–1053.
McDonald, F.B., Williams, R., Sheehan, D., O'Halloran, K.D., 2015. Early life exposure to chronic intermittent hypoxia causes upper airway dilator muscle weakness, which persists into young adulthood. Exp. Physiol. 100, 947–966.
Menuet, C., Borghgraef, P., Matarazzo, V., Gielis, L., Lajard, A.M., Voituron, N., Gestreau, C., Dutschmann, M., Van Leuven, F., Hilaire, G., 2011a. Raphe tauopathy alters serotonin metabolism and breathing activity in terminal tau.P301L mice: possible implications for tauopathies and Alzheimer's disease. Respir. Physiol. Neurobiol. 178, 290–303.
Menuet, C., Cazals, Y., Gestreau, C., Borghgraef, P., Gielis, L., Dutschmann, M., Van Leuven, F., Hilaire, G., 2011b. Age-related impairment of ultrasonic vocalization in tau.P301L mice: possible implication for progressive language disorders. PLoS One 6, e25770.
Mishra, S.K., Singh, S., Shukla, S., Shukla, R., 2017. Intracerebroventricular streptozotocin impairs adult neurogenesis and cognitive functions via regulating neuroinflammation and insulin signaling in adult rats. Neurochem. Int. 113, 56–68.
Mitchell, S.L., Teno, J.M., Kiely, D.K., Shaffer, M.L., Jones, R.N., Prigerson, H.G., Volicer, L., Givens, J.L., Hamel, M.B., 2009. The clinical course of advanced dementia. N. Engl. J. Med. 361, 1529–1538.
Newman, A.B., Fitzpatrick, A.L., Lopez, O., Jackson, S., Lyketsos, C., Jagust, W., Ives, D., Dekosky, S.T., Kuller, L.H., 2005. Dementia and Alzheimer's disease incidence in relationship to cardiovascular disease in the cardiovascular health study cohort. J. Am. Geriatr. Soc. 53, 1101–1107.
O'Halloran, K.D., 2016. Chronic intermittent hypoxia creates the perfect storm with calamitous consequences for respiratory control. Respir. Physiol. Neurobiol. 226, 63–67.
Osorio, R.S., Gumb, T., Pirraglia, E., Varga, A.W., Lu, S.E., Lim, J., Wohlleber, M.E., Ducca, E.L., Koushyk, V., Glodzik, L., Mosconi, L., Ayappa, I., Rapoport, D.M., de Leon, M.J., 2015. Sleep-disordered breathing advances cognitive decline in the elderly. Neurology 84, 1964–1971.
Pan, W., Kastin, A.J., 2014. Can sleep apnea cause Alzheimer's disease? Neurosci. Biobehav. Rev. 47, 656–669.
Saraceno, C., Musardo, S., Marcello, E., Pelucchi, S., Di Luca, M., 2013. Modeling Alzheimer's disease: from past to future. Front. Pharmacol. 4, 77.
Secil, Y., Arici, S., Incesu, T.K., Gurgor, N., Beckmann, Y., Ertekin, C., 2016. Dysphagia in Alzheimer's disease. Neurophysiol. Clin. 46, 171–178.
Simic, G., Stanic, G., Mladinov, M., Jovanov-Milosevic, N., Kostovic, I., Hof, P.R., 2009. Does Alzheimer's disease begin in the brainstem? Neuropathol. Appl. Neurobiol. 35, 532–554.
Skelly, J.R., Edge, D., Shortt, C.M., Jones, J.F., Bradford, A., O'Halloran, K.D., 2012. Tempol ameliorates pharyngeal dilator muscle dysfunction in a rodent model of chronic intermittent hypoxia. Am. J. Respir. Cell Mol. Biol. 46, 139–148.
Souza, G.M., Bonagamba, L.G., Amorim, M.R., Moraes, D.J., Machado, B.H., 2015. Cardiovascular and respiratory responses to chronic intermittent hypoxia in adult female rats. Exp. Physiol. 100, 249–258.
Souza, L.C., Jesse, C.R., Del Fabbro, L., de Gomes, M.G., Gomes, N.S., Filho, C.B., Goes, A.T.R., Wilhelm, E.A., Luchese, C., Roman, S.S., Boeira, S.P., 2018. Aging exacerbates cognitive and anxiety alterations induced by an intracerebroventricular injection of amyloid-beta1-42 peptide in mice. Mol. Cell. Neurosci. 88, 93–106.
Stewart, S.A., German, R.Z., 1999. Sexual dimorphism and ontogenetic allometry of soft tissues in rattus norvegicus. J. Morphol. 242, 57–66.
Takenoshita, S., Kondo, K., Okazaki, K., Hirao, A., Takayama, K., Hirayama, K., Asaba, H., Nakata, K., Ishizu, H., Takahashi, H., Nakashima-Yasuda, H., Sakurada, Y., Fujikawa, K., Yokota, O., Yamada, N., Terada, S., Middle Western Japan-Dementia, S, 2017. Tube feeding decreases pneumonia rate in patients with severe dementia: comparison between pre- and post-intervention. BMC Geriatr. 17, 267.
Teran, F.A., Massey, C.A., Richerson, G.B., 2014. Serotonin neurons and central respiratory chemoreception: where are we now? Prog. Brain Res. 209, 207–233.
van der Steen, J.T., Mehr, D.R., Kruse, R.L., Sherman, A.K., Madsen, R.W., D'Agostino, R.B., Ooms, M.E., van der Wal, G., Ribbe, M.W., 2006. Predictors of mortality for lower respiratory infections in nursing home residents with dementia were validated transnationally. J. Clin. Epidemiol. 59, 970–979.
Van Eldik, L.J., Carrillo, M.C., Cole, P.E., Feuerbach, D., Greenberg, B.D., Hendrix, J.A., Kennedy, M., Kozauer, N., Margolin, R.A., Molinuevo, J.L., Mueller, R., Ransohoff, R.M., Wilcock, D.M., Bain, L., Bales, K., 2016. The roles of inflammation and immune mechanisms in Alzheimer's disease. Alzheimers Dement. (N. Y.) 2, 99–109.
Yagishita, S., Suzuki, S., Yoshikawa, K., Iida, K., Hirata, A., Suzuki, M., Takashima, A., Maruyama, K., Hirasawa, A., Awaji, T., 2017. Treatment of intermittent hypoxia increases phosphorylated tau in the hippocampus via biological processes common to aging. Mol. Brain 10, 2.